



**HAL**  
open science

## Tunable resonators in the low kHz range for viscosity sensing

Martin Heinisch, Erwin Reichel, Isabelle Dufour, Bernhard Jakoby

► **To cite this version:**

Martin Heinisch, Erwin Reichel, Isabelle Dufour, Bernhard Jakoby. Tunable resonators in the low kHz range for viscosity sensing. *Sensors and Actuators A: Physical*, 2012, 186, pp.111-117. 10.1016/j.sna.2012.03.009 . hal-00676516

**HAL Id: hal-00676516**

**<https://hal.science/hal-00676516v1>**

Submitted on 13 Nov 2014

**HAL** is a multi-disciplinary open access archive for the deposit and dissemination of scientific research documents, whether they are published or not. The documents may come from teaching and research institutions in France or abroad, or from public or private research centers.

L'archive ouverte pluridisciplinaire **HAL**, est destinée au dépôt et à la diffusion de documents scientifiques de niveau recherche, publiés ou non, émanant des établissements d'enseignement et de recherche français ou étrangers, des laboratoires publics ou privés.

# Tunable resonators in the low kHz range for viscosity sensing

M. Heinisch<sup>a</sup>, E.K. Reichel<sup>b</sup>, I. Dufour<sup>c</sup>, B. Jakoby<sup>a</sup>

<sup>a</sup>Institute for Microelectronics and Microsensors, Johannes Kepler University, Linz, Austria

<sup>b</sup>Center for Surface Science and Catalysis, Katholieke Universiteit Leuven, Belgium

<sup>c</sup>Université de Bordeaux, Laboratoire de l'Intégration du Matériau au Système, France

---

## Abstract

This contribution gives an overview of the design and development of miniaturized, tunable resonating viscosity sensors in the low kHz range incorporating first modeling approaches as well as experimental results. The effect of different designs, potential improvements in the setups as well as the effect of cross sensitivities are discussed and outlined.

*Keywords:* viscosity, mass density, sensor, frequency, Lorentz forces

---

## 1. Introduction

Miniaturized viscosity sensors are attractive devices for condition monitoring applications involving fluid media. Most recently introduced devices utilize vibrating resonant mechanical structures interacting with the fluid where the resonant behavior (resonance frequency and quality factor) is affected by the fluid's mass density and viscosity [1, 2]. So far, the ability of tuning the resonance frequency of such devices in a larger frequency range has hardly been reported. However, such a feature is highly desirable particularly when investigating complex liquids showing viscoelastic behavior. We devised two different types of resonating viscosity sensors with tunable resonance frequencies in a range of over two octaves for a fixed geometry. Analytical models relating measured data to the viscosity of the examined liquid have been presented earlier together with first measurement data where we briefly discussed the benefits of different geometries in terms of high tunability and their sensitivity to viscosity [3, 4, 5].

Complex fluids often show viscoelastic behavior which means that they exhibit a significant frequency dependence in their shear modulus (whose imaginary part is related to the shear viscosity) when using oscillatory rheometers. Laboratory rheometers work in a limited frequency range not exceeding typically 100 Hz and commonly, they are not suitable for online monitoring applications as they are expensive and maintenance intensive (e.g., due to macroscopically moving parts involving bearings etc.). Miniaturized devices sensing viscosity in the MHz range have been discussed extensively in the past, e.g. thickness shear mode resonators [6]. Between these devices, providing a "high-frequency viscosity" and the aforementioned laboratory viscometers is a gap, which we are aiming to bridge with devices as presented in this contribution.

Recently, we proposed a design for a tunable in-plane resonating sensor for viscosity [3]. As an alternative, a single wire device has been investigated [4]. Both types of these resonating sensors provide a large range of achievable resonance frequencies (over two octaves up to  $\sim 4$  kHz for our first devices with a

fixed vibrating length of  $\sim 3$  cm). The tuning of the resonance frequency is achieved by the variation of tensile stresses in the wires by an appropriate tensioning mechanism.

These and previously reported sensors (e.g., [7]) underlie the same principles of actuation and read out, namely actuation by means of Lorentz forces  $F_L$  and read out via the (motion) induced voltage  $V_M$ , where

$$dF_L = I_{in} B dl_a \quad (1)$$

( $I_{in}$ : sinusoidal input (driving) current,  $B$ : magnetic flux density provided by a permanent magnet (assembly),  $l_a$ : length of the electrical conductive path used for actuation) and

$$dV_M = v B dl_{ro} \quad (2)$$

( $v$ : velocity of the electrical conductive path used for read out,  $l_{ro}$ : length of the readout path) Here, orthogonality of the direction of the current flow,  $B$  and  $v$  was assumed.

The motion induced voltage is the quantity representing the resonator's movement in the fluid-structure interaction (FSI) which is thus related to the fluid's dynamic viscosity for a known mass density (and vice versa).

This contribution explains the principles and the physical relations (by means of closed form models) of the Suspended Plate and the Wire Viscometer in Sec. 2 and 3, respectively. Section 4 briefly shows experimental results revealing both sensors' response (and sensitivity) to viscosity. The following section focuses on the tunability of the resonance frequencies of both resonators, see Sec. 5. Based on these first (feasibility) concepts discussed in the aforementioned sections, this work is extended by several (indispensable) improvement strategies effecting higher readout signals and more reliable setups allowing for more accurate sensing, see Sec. 6.

## 2. Suspended Plate Viscometer

### 2.1. Setup

The principle of the Suspended Plate Viscometer (which is fully surrounded by the sample liquid) is depicted in Fig.1(a).

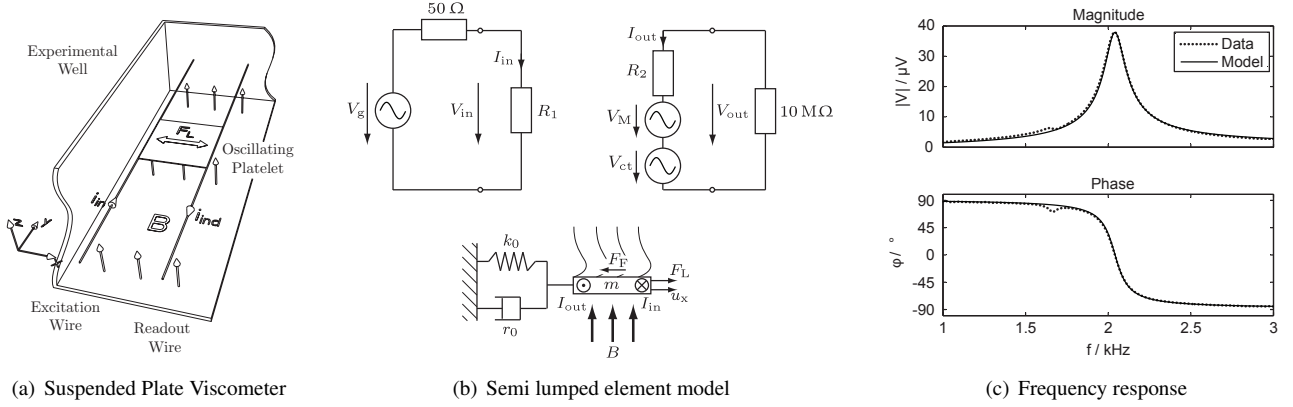


Figure 1: In (a) a schematic drawing of the suspended plate rheometer is depicted. The sensor, surrounded by an experimental well, consists of two parallel wires (placed in external field  $\mathbf{B}$ ) and a small platelet. In this figure, the left wire is used for exciting lateral vibrations by means of Lorentz forces. The second wire on the right used for pick-up, is coupled to the excitation wire with a rigid plate, thus following the movement of the left wire which effects an induced voltage which is used as read-out. By changing the tensile stresses in the wires, the resonance frequency can be changed. In (b) the scheme of the modeling approach is depicted. The upper figure shows the electrical equivalent circuit consisting of two galvanically isolated circuits representing the excitation and read-out circuits. ( $V_g$ : Voltage of the function generator,  $50 \Omega$ : Internal resistance of the function generator,  $R_1$ : resistance of the excitation wire,  $R_2$ : resistance of the pick-up wire,  $V_M$ : Motion induced voltage,  $V_{ct}$ : Induced voltage through electrical cross-talk,  $10 M\Omega$ : Input resistance of the lock-in amplifier,  $I_{in}$ ,  $I_{out}$ ,  $V_{in}$ ,  $V_{out}$ : Input and output currents / voltages). The lower figure shows the mechanical lumped-element model. ( $k_0$ : intrinsic spring constant,  $r_0$ : intrinsic damping parameter,  $F_F$ : Fluid forces,  $F_L$ : Lorentz forces,  $u_x$ : displacement in  $x$ -direction,  $B$ : external magnetic field). In (c) a comparison between measured data (in this case for isopropanol) and the model obtained by fitting the parameters from Eq. 6 is shown.

A small platelet which is suspended by two wires is forced to lateral vibrations by means of Lorentz forces on AC-currents in the excitation wire. This in-plane fluid-structure interaction of the platelet with the surrounding liquid is recorded via the motion induced voltage in the second wire which follows the movement of the platelet (and the excitation wire). Varying the tensile stresses within both wires (by an appropriate tensioning mechanism) allows for setting the desired resonance frequency (in a given bandwidth, see Sec. 5).

In first setups,  $100 \mu\text{m}$  thick tungsten wires were used (because of tungsten's high ultimate strength exceeding  $1.5 \text{ GPa}$ ). For the platelet's material glass or PET was used which yielded both good results and mainly differed in the fabrication technique, see [3]. Similar designs have also been fabricated using one material only (nickel brass) and their tunability was briefly investigated but has not been published yet. Resonating platelets made of one material only and fabricated with micro-machining techniques are reported e.g., in [8, 9].

## 2.2. Semi lumped element model

As the platelet's lateral dimensions are much larger than its thickness and as its surface  $A$  is much larger than the wire's surfaces, boundary effects emerging from displacement of the liquid at the platelets front sides as well as the flow around the wires are not taken into account. The fluid forces  $F_F$  acting on the platelet are modeled by one-dimensional shear wave propagation,

$$F_F = -2T(z=0)A \quad (3)$$

where the shear stress is [3, 6] (using complex notation assuming time dependence  $e^{j\omega t}$ )

$$T(z=0) = u_x(1-j)\sqrt{\frac{\mu\rho\omega^3}{2}} \quad (4)$$

With this, the transfer function of the mechanical oscillator, which is the quotient of displacement in  $x$ -direction  $u_x$  and Lorentz forces Eq. 1 can be written as (see also Fig. 1(b) and Eq. 1)

$$G_m = \frac{u_x}{F_L} \quad (5)$$

$$= \frac{1}{-\omega^2 \left( m + A \sqrt{\frac{\mu\rho}{2\omega}} \right) + j\omega \left( r_0 + A \sqrt{\frac{\mu\rho\omega}{2}} \right) + k_0}$$

Finally, the motion-induced voltage (see Eq. 2) in the pickup wire can be written as follows

$$V_M = j\omega G_m \frac{B^2 l_a^* l_{ro}^*}{R_1} V_{in} \quad (6)$$

here,  $l_a^*$  and  $l_{ro}^*$  are the wire's effective lengths (which depend on the mode shape but are in the order of the actual length).

It may be necessary to consider the effect of electrical cross-talk in the measured voltage as well, see [10], which can be easily taken into account with

$$V_{ct} = \frac{j\omega M}{R_1} V_{in} \quad (7)$$

where  $M$  is the mutual inductance describing the inductive coupling between excitation and read-out circuit. As the input resistance of the lock-in amplifier is  $10 M\Omega$ , it is assumed that  $I_{out} \approx 0$  and thus the total amount of output voltage is given by

$$V_{out} = V_M + V_{ct} \quad (8)$$

A comparison between this simple (fitted) model and measured data for isopropanol is shown in Fig. 1(c).

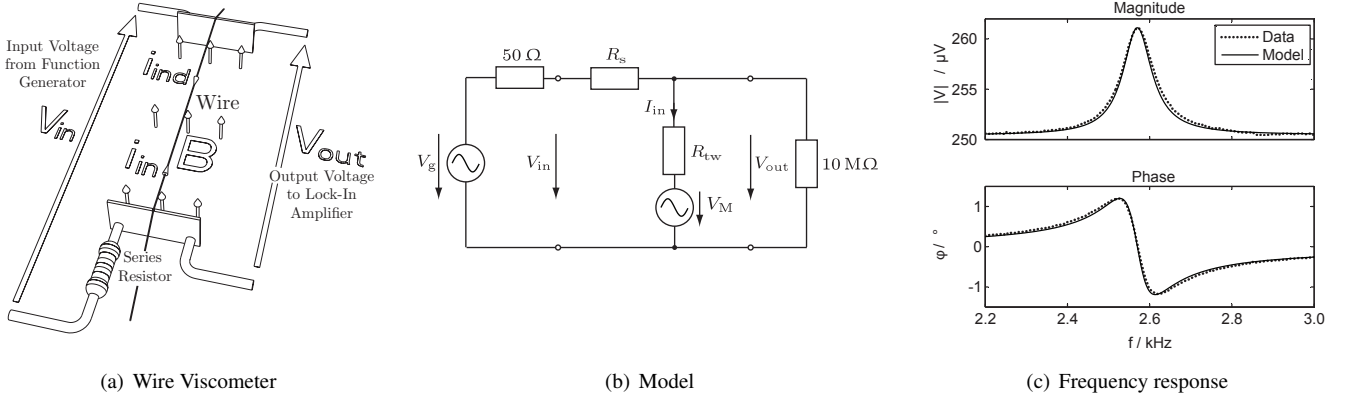


Figure 2: In (a) the schematic drawing of the wire viscometer is depicted. The experimental well for investigating sample liquids is not shown in this sketch. A 100  $\mu\text{m}$  thick tungsten wire carrying sinusoidal currents is placed in an external magnetic field and thus oscillating due to Lorentz forces. For excitation, a function generator is used for the input signal. A series resistor is used to limit the excitation current. The motion induced voltage (i.e., the read-out signal) is measured with lock-in amplifier. The resonance frequency can be changed by (mechanically) changing the tensile stresses in the wire. In (b) the electrical equivalent circuit of the wire viscometer is illustrated. ( $R_s$ : series resistor to limit the excitation current,  $R_{tw}$ : resistance of the tungsten wire). In (c) a comparison between measured data (in this case for isopropanol) and the model obtained by fitting the parameters from Eq. 14 is shown.

### 3. Wire Viscometer

Resonating viscometers using a single wire only, are known as wire viscometers in literature [11, 12, 13]. These viscometers were designed to be operated at one fixed resonance frequency only. In our work, we focus on the investigation of tuning the resonance frequencies of the vibrating sensors within a preferentially large range and focus on miniaturized devices.

#### 3.1. Setup

Figure 2(a) shows a schematic sketch of the wire viscometer. A tungsten wire is stretched over two electrical conductive blades. For first (test) setups these blades, determining the vibrating length and assuring for electrical contact, were made of PCB (copper coated fiberglass) which were later replaced by machined metal blades, see Sec. 6. The series resistor limits the excitation current to avoid non linear effects such as e.g., Duffing behavior, see [13]. For measurements in air about 10 k $\Omega$  and in liquids, resistors between 50  $\Omega$  and 1 k $\Omega$  were used. The external magnetic field was generated with different Nd-FeB magnet assemblies yielding magnetic flux densities from 0.3 T up to 1.4 T, see [14].

#### 3.2. Modeling

For the modeling of the wire viscometer, the transversal movements  $w(x, t)$  of the wire subjected to an axial force  $N$ , driving Lorentz forces  $F_L$  and the loading of the fluid forces  $F_F$  can be described by the following linear, inhomogenous, partial differential equation in time domain [15, 16]:

$$E I \frac{\partial^4 w(x, t)}{\partial x^4} - N \frac{\partial^2 w(x, t)}{\partial x^2} + m' \frac{\partial^2 w(x, t)}{\partial t^2} = F_L'(x, t) + F_F'(x, t) \quad (9)$$

( $E$ : Young's modulus,  $I$ : second moment of inertia,  $m'$ : wire's mass,  $'$ : quantity in respect of unit length)

Eq. 9 is transformed to the frequency domain again assuming a time dependence  $e^{j\omega t}$  and the forces per unit length on the

right hand side of Eq. 9 acting on the wire are substituted by the following expressions

$$F_L' = I_{in}(\omega) B \quad (10)$$

and from [17]:

$$F_F'(x, \omega) = -j\omega g_1(x, \omega) w(x, \omega) + \omega^2 g_2(x, \omega) w(x, \omega) \quad (11)$$

( $I_{in}$ : input current,  $B$ : flux density of the external magnetic field which is provided by a permanent magnet,  $\omega$ : angular frequency of the harmonic oscillation)  $g_1$  and  $g_2$  can be calculated by using the analytical relation of the fluid forces acting on a circular cylinder [18], [19]:

$$F_F'(x, \omega) = \pi \rho_f \omega^2 R^2 \left( 1 - \frac{4 j K_1(j \sqrt{-j Re})}{\sqrt{-j Re} K_0(j \sqrt{-j Re})} \right) w(x, \omega) \quad (12)$$

$$\text{where } Re = \frac{\rho \omega R^2}{\mu} \quad (13)$$

( $R$ : wire radius,  $K_0$ ,  $K_1$ : modified Bessel functions,  $\mu$ : dynamic viscosity) After the analytical calculation of the deflection of the wire  $w(x, \omega)$ , the induced voltage is calculated as follows:

$$V_{out} = j \omega B \int_0^l w(x, \omega) dx + R_{tw} I_{in}(\omega) \quad (14)$$

( $l$ : wire length,  $R_{tw}$ : wire ohmic resistance) Fig.2(c) shows a comparison of measurement data and a fit of this model.

### 4. Response to viscosity

From the resonant behavior (which is monitored by the motion induced voltage in the wire) the viscosity of a sample liquid is determined (knowing the liquid's mass density).

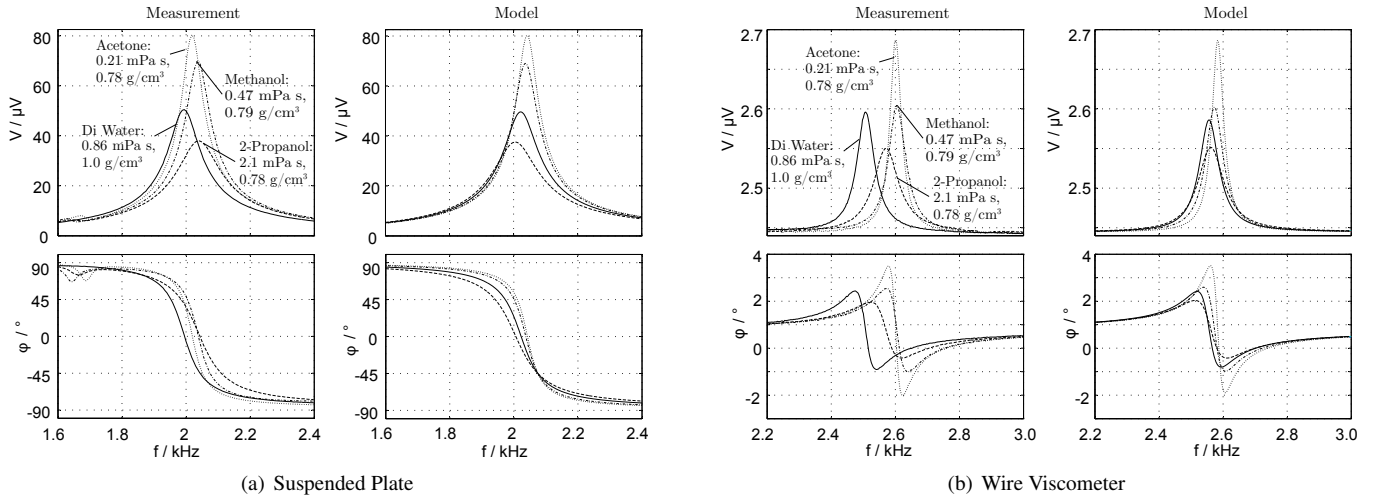


Figure 3: In both figures the sensors measured and theoretical frequency responses including the fundamental harmonic in four different liquids are illustrated (Excitation Voltage  $V_g=0.5V$ ). For both sensors, clearly, it is visible that higher viscosities yield higher damping. The effect of the the viscosity and the mass density on the resonance frequency shift can be observed in the according theoretical frequency responses. The deviation in the resonance frequencies between model and experiment are mainly caused by undesired de-tuning of the sensor.

The effect of different viscosities on the resonant behavior was examined by recording the frequency response including the fundamental mode in four different liquids. The selected liquids only have small differences in their viscosity, ranging from 0.21 mPa s to 2.1 mPa s to investigate the sensitivity to viscosity. The used liquids were acetone, methanol, isopropanol and DI-water, see Fig.3. The indicated reference values for viscosity and mass-density were measured with a Stabinger Viscometer (SVM 3000) at 25 °C.

For the measurements in this study, we observed shifts in the resonance frequencies, see Fig. 3, which are mainly not caused by the different physical properties of the liquids but by de-tuning of the sensor (e.g., from thermal stresses, slacking of the entire setup, etc.). However the liquid’s physical properties (theoretically) have a significant effect on the shift of the resonance frequency which can nicely be observed in the heoretical frequency responses in Fig. 3. From these theoretical frequency responses it can also bee seen, that the wire viscometer is more sensitive to mass density. (Compare the theoretical frequency responses of water, which has a higher mass density than the examined solvents.)

For obtaining these theoretical frequency responses, the models described in Sec. 2.2 and 3.2 were compared to the four measured frequency responses. In the theoretical evaluation of the wire viscometer and the suspended plate sensor the normal stresses and the intrinsic spring constant, respectively, were kept constant to show the effect of the physical properties on the frequency shift.

Based on the insights gained with these measurements, we aim at setups yielding stable resonance frequencies, see discussion in Sec. 6, for accurate and reliable sensing.

#### 4.1. Discussion and comparison

For a rough estimate, to compare the sensors’ sensitivity to viscosity, we evaluated the Q-factors  $Q = f_r/(f_+ - f_-)$  when

the sensors were immersed in the different sample liquids detecting the maximum and -3 dB values in the magnitude of the frequency response for both, the measured and the theoretical frequency responses. Both sensors show a similar sensitivity to viscosity when evaluating their quality factors in the examined range of viscosity, see Fig. 4. We note that with the wire viscometer it is in principle possible to measure both, mass density and viscosity with a single measurement only, however, with restricted accuracy [12]. The sensitivity of the wire viscometer to mass density can be observed in the theoretic frequency response in Fig. 3(b). There, the shift of the resonance frequency is mainly affected by the mass density which is nicely visible for the case of water which has a higher mass density than the other examined liquids.

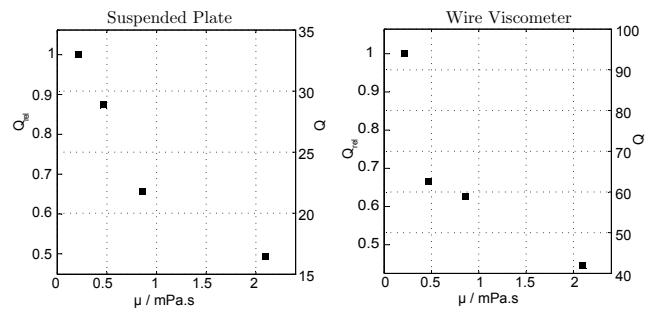


Figure 4: Comparison of the Q-factor. For both sensors, the relative and the absolute values are indicated. In the investigated range, both sensors show a similar sensitivity to viscosity. The two dashed lines in both figures show the theoretical results for the Q-factor for the indicated mass densities.

### 5. Tunability of the resonance frequency

To show the capability of the tuning of the resonance frequency the normal stresses in the wires were changed by tensioning the wires with micro-stages with micrometer screws.

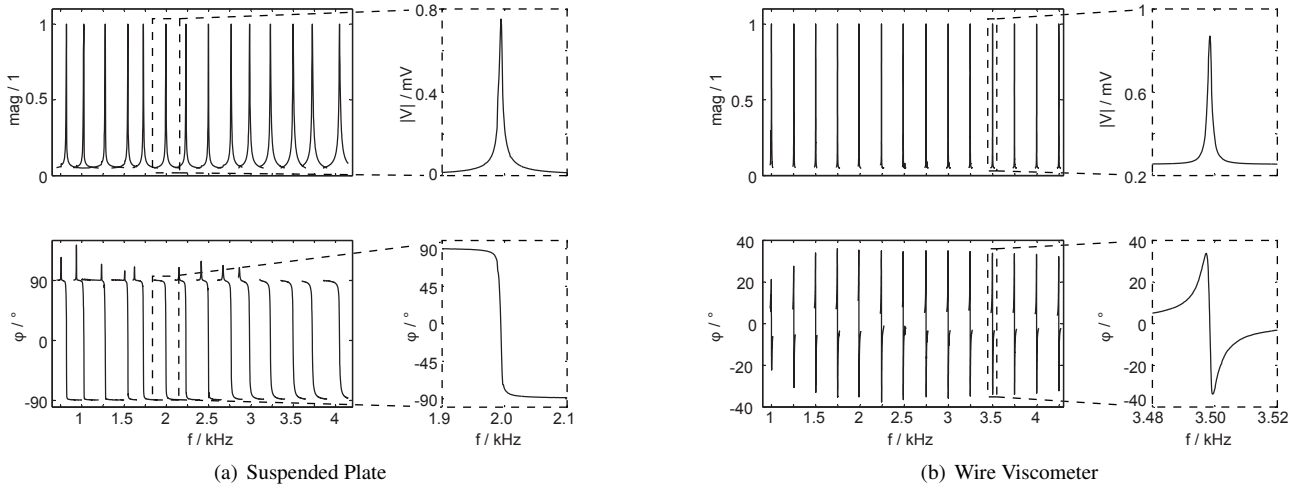


Figure 5: In both figures the band width of achievable resonance frequencies (in air) using 3 cm long and 100  $\mu\text{m}$  thick tungsten wires are illustrated. In each case a detailed view of one characteristic resonance is depicted as well. In case (b) (wire viscometer) higher quality factors are obtained. (Note that the bandwidths in the detailed views are 40 Hz for the wire viscometer and 200 Hz for the suspended plate rheometer.) The obtained resonances in first measurements go from 1000 Hz to 4250 Hz in case of the wire viscometer and from 820 Hz to 4040 Hz for the suspended plate rheometer. In both cases, for changing the resonance frequencies for these measurements, the normal stresses in the wires were varied by tensioning the wires with micro-stages with micrometer screws.

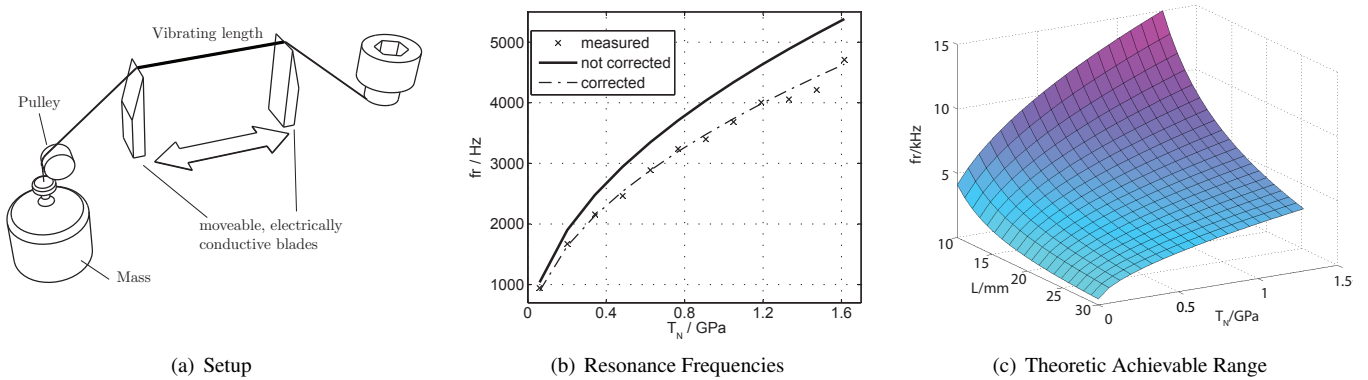


Figure 6: In (a) a setup of the wire viscometer allowing for changing both, the normal stresses in the wire as well as its length is depicted. A tungsten wire is placed in an external magnetic field (not depicted; perpendicular to the wire). The conductive blades allow for electrical contact and for changing the wire's vibrating length. One end of the wire is rigidly affixed. The other is attached to a weight, which is varied for changing the normal stresses in the wire but keeping the normal stresses constant when changing the vibrating length. (b) Comparison of measured and theoretic resonance frequencies for different normal stresses  $N$ . The solid line shows the theoretic results obtained by using the given material parameters, whereas for the dashed line, these parameters were fitted. In (c) the results from a theoretical estimation of achievable resonance frequencies, when changing the normal stresses as well as the wire's vibrating length for a 100  $\mu\text{m}$  thick tungsten wire with  $L = 10 \dots 30$  mm and  $T_N = 0 \dots 1.4$  GPa is depicted. (Tungsten has a yield stress of 1.5 GPa, approximately)

In first experiments in air resonances between 1000 Hz and 4250 Hz in case of the wire viscometer and 820 Hz and 4040 Hz in case of the suspended plate rheometer were achieved, see Fig. 5, [4]. The intention of these experiments was to monitor which frequency range can be excited.

With a second experiment, see Fig. 6(a), we wanted to further investigate the achievable tunable range for the case of an oscillating wire when varying both, normal stresses as well as the vibrating length of the wire. Figure 6(b) shows the results for the experiment for a constant length  $l = 30$  mm for different normal stresses in the wire, which shows the same range of resonance frequencies as in the first experiment, c.f., Fig. 5(b). A relatively large deviation of measured resonance frequencies to the theoretical values can be observed. This deviation results

from frictional forces between the blades and the wire. That is to say that not the total amount of normal forces (provided by the weight) is transferred to the vibrating part of the wire, but that instead they are partially balanced at the blades due to frictional forces. This assumption was confirmed by a further experiment, see Sec. 6 below.

Figure 6(c) shows the (theoretically) total achievable range of resonance frequencies when changing the normal stresses as well as the wire's vibrating length for a 100  $\mu\text{m}$  thick tungsten wire with the limiting factors  $L = 10 \dots 30$  mm and  $T_N = 0 \dots 1.4$  GPa. This range has been verified experimentally and good accordance was observed.



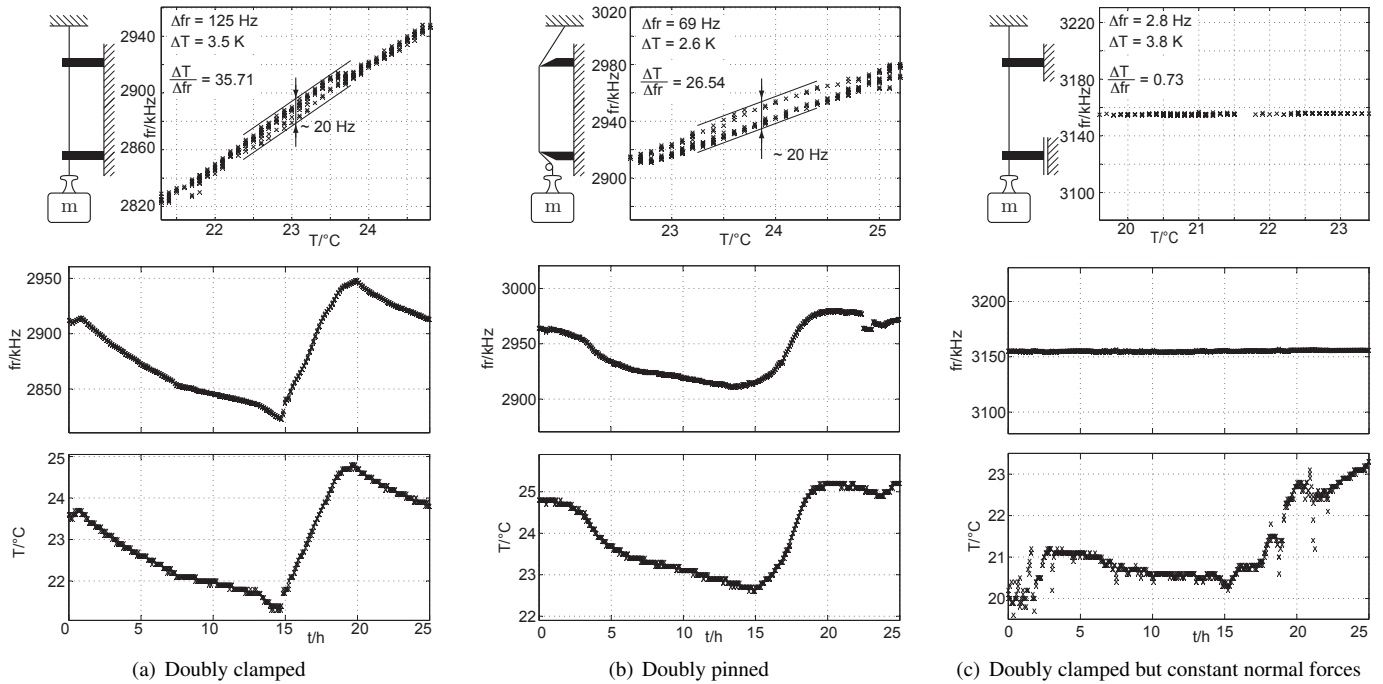


Figure 7: Effect of three different types of wire clamping on the resonance frequency. For each case the resonance frequency over temperature as well as resonance frequency and temperature over time is plotted.

## 6. Improved setups using the Wire Viscometer as example

### 6.1. Reducing cross sensitivities

The previous sections showed a proof of concept of both types of sensors. They are well applicable for viscosity sensing and can be detuned in a range of over one decade. However, from the first experiments, it became clear that several improvements have to be achieved, which we want to discuss for the example of the wire viscometer. In this contribution we focus on the discussion on improving the stability of the resonance frequency (once it is set to a desired value). In [14] a discrete permanent magnet assembly is presented yielding a flux density of 1.2 T in a 4 mm airgap, which drastically improves the magnitude of the read-out signal.

We investigated three different types of wire clamping, see Fig. 7, in the laboratory during 25 hours recording the ambient temperature to study the range of resonance frequency changes under (randomly) varying conditions in a non-air-conditioned room. For the first case (Fig. 7(a)) we expected high shifts of the resonance frequency due to thermal stresses resulting from the different thermal expansion coefficient of the used materials. The problematic characteristic of setup (a) is not (only) this high temperature dependency but that for a given temperature the variation of resonance frequencies is still about 20 Hz. Thus the idea was to keep the normal stresses constant by pinning the wire instead of clamping, see Fig. 7(b). However, in this case, there is still a relatively large temperature dependency which can only be explained with friction forces between the blades and the wire, c.f. discussion in Sec. 5. Here, also a significant hysteresis can be observed within a temperature cycle. In the third setup, see Fig. 7(c) an almost frictionless linear stage was

used to keep the normal stresses in the clamped wire as constant as possible. With this setup the variation of the resonance frequency is less than 3 Hz and mainly not dependent on the ambient temperature.

## 7. Conclusion

This work shows the feasibility of measuring viscosity with both presented sensors at tunable resonance frequencies. For the case of the wire viscometer an improved setup has been found allowing for stable resonance frequencies. Furthermore, first closed-form models have been developed which can be fitted into the measured data with high accuracy. Regarding future work, the stability of both sensors has to be investigated and most likely, improved with more sophisticated setups. For this investigation large measurement series with multiple test liquids over a long period of time have to be carried out.

## 8. Acknowledgement

We are indebted to the Austrian Competence Centre of Mechatronics (ACCM) for the financial support.

## References

- [1] Jakoby, R. Beigelbeck, F. Keplinger, F. Lucklum, A. Niedermayer, E. Reichel, C. Riesch, T. Voglhuber-Brunnmaier, B. Weiss, Miniaturized sensors for the viscosity and density of liquids – performance and issues, ITUCER 57 (1). doi:10.1109/TUFFC.2010.1386.
- [2] C. Riesch, E. Reichel, A. Jachimowicz, J. Schalko, P. Hudek, B. Jakoby, F. Keplinger, A suspended plate viscosity sensor featuring in-plane vibration and piezoresistive readout, J. Micromech. Microeng. 19. doi:10.1088/0960-1317/19/7/075010.

- [3] M. Heinisch, E. Reichel, B. Jakoby, A suspended plate in-plane resonator for rheological measurements at tunable frequencies, in: Proc. Sensor + Test, 2011, pp. 61–66.
- [4] M. Heinisch, E. Reichel, B. Jakoby, A study on tunable resonators for rheological measurements, in: Proc. SPIE, Vol. 8066, 2011. doi:10.1117/12.887103.
- [5] M. Heinisch, E. Reichel, I. Dufour, B. Jakoby, Miniaturized resonating viscometers facilitating measurements at tunable frequencies in the low khz-range, in: Proc. Eurosensors, 2011.
- [6] S. Martin, V. E. Granstaff, G. C. Frye, Characterization of a quartz crystal microbalance with simultaneous mass and liquid loading, in: Anal. Chem., Vol. 63, 1991, pp. 2272–2281.
- [7] M. Heinisch, E. Reichel, I. Dufour, B. Jakoby, A resonating rheometer using two polymer membranes for measuring liquid viscosity and mass density, Sens. Actuators A: Physdoi:10.1016/j.sna.2011.02.031.
- [8] E. Reichel, C. Riesch, F. Keplinger, C. Kirschhock, B. Jakoby, Analysis and experimental verification of a metallic suspended plate resonator for viscosity sensing, Sensors and Actuators A: Physical 162 (2010) 418–424. doi:10.1016/j.sna.2010.02.017.
- [9] E. Reichel, J. Vermant, B. Jakoby, C. Kirschhock, Shear wave sensors for viscoelastic properties, in: Procedia Engineering, Vol. 5, 2010, pp. 1316–1319. doi:10.1016/j.proeng.2010.09.356.
- [10] M. Heinisch, E. Reichel, B. Jakoby, A feasibility study on tunable resonators for rheological measurements, in: Proceedings GMe Forum, 2011, pp. 85–89.
- [11] T. Retsina, S. M. Richardson, W. A. Wakeham, The theory of a vibrating-rod viscometer, Applied Scientific Research 4 (1986) 325–346. doi:10.1007/BF00540567.
- [12] D. Seibt, Schwingdrahtviskosimeter mit integriertem Einsenkkorperdichtemessverfahren fur Untersuchungen an Gasen in groseren Temperatur- und Druckbereichen, Ph.D. thesis, Universitat Rostock (2007).
- [13] M. Sullivan, C. Harrison, A. Goodwin, K. Hsu, S. Godefroy, On the nonlinear interpretation of a vibrating wire viscometer operated at large amplitude, Fluid Phase Equilibria 276 (2009) 99–107. doi:10.1016/j.fluid.2008.10.017.
- [14] M.Heinisch,E.Reichel,I.Dufour,B.Jakoby,Tunableminiaturizedviscosity sensors operating in the khz-range, in: Proc. IEEE Sensors, 2011.
- [15] W.Weaver,S.Timoshenko,D.Young,Vibration Problems inEngineering, 5th Edition, Wiley, 1990.
- [16] M. Elwenspoek, R. Wiegerink, Mechanical Microsensors, Springer-Verlag, 2001.
- [17] L.D.Landau, E.M.Lifshitz, Fluid Mechanics, Butterworth-Heinemann, 1987.
- [18] L.Rosenhead,LaminarBoundaryLayers,Clarendon,Oxford,1963.
- [19] J.Sader,Frequency response of cantilever beams immersed in viscous fluids with applications to the atomic force microscope, Journal of Applied Physics 84 (1998) 64 – 76.

## Biographies

**Martin Heinisch** obtained his Dipl.-Ing. (M.Sc.) in Mechatronics from Johannes Kepler University Linz, Austria, in 2009. After his Master studies he went to the University of California, Los Angeles (U.C.L.A.) as a Marshall Plan Scholarship grantee, where he did research in the field of microfluidic applications and self assembling systems. In 2010 he started a Ph.D. program at the Institute for Microelectronics and Microsensors of the Johannes Kepler University Linz, Austria where he is currently working on resonating liquid sensors.

**Erwin K. Reichel** was born in Linz, Austria, in 1979. He received the Dipl.-Ing. (M.Sc.) degree in mechatronics from Johannes Kepler University, Linz, Austria, in 2006. From 2006 to 2009 he was working on the Ph.D. thesis at the Institute for Microelectronics and Microsensors of the Johannes Kepler University, Linz. In 2009 he obtained his doctoral (Ph.D.) degree

and now holds a post-doctoral position at the Centre for Surface Chemistry and Catalysis, KU Leuven, Belgium. The main research fields are the modeling, design, and implementation of sensors for liquid properties, and monitoring of phase transition in complex solutions.

**Isabelle Dufour** graduated from Ecole Normale Supérieure de Cachan in 1990 and received the Ph.D. and H.D.R. degrees in engineering science from the University of Paris-Sud, Orsay, France, in 1993 and 2000, respectively. She was a CNRS research fellow from 1994 to 2007, first in Cachan working on the modelling of electrostatic actuators (micromotors, micropumps) and then after 2000 in Bordeaux working on microcantilever-based chemical sensors. She is currently Professor of electrical engineering at the University of Bordeaux and her research interests are in the areas of microcantilever-based sensors for chemical detection, rheological measurements and materials characterisation.

**Bernhard Jakoby** obtained his Dipl.-Ing. (M.Sc.) in Communication Engineering and his doctoral (Ph.D.) degree in electrical engineering from the Vienna University of Technology (VUT), Austria, in 1991 and 1994, respectively. In 2001 he obtained a *venia legendi* for Theoretical Electrical Engineering from the VUT. From 1991 to 1994 he worked as a Research Assistant at the Institute of General Electrical Engineering and Electronics of the VUT. Subsequently he stayed as an Erwin Schrödinger Fellow at the University of Ghent, Belgium, performing research on the electrodynamics of complex media. From 1996 to 1999 he held the position of a Research Associate and later Assistant Professor at the Delft University of Technology, The Netherlands, working in the field of microacoustic sensors. From 1999 to 2001 he was with the Automotive Electronics Division of the Robert Bosch GmbH, Germany, where he conducted development projects in the field of automotive liquid sensors. In 2001 he joined the newly formed Industrial Sensor Systems group of the VUT as an Associate Professor. In 2005 he was appointed Full Professor of Microelectronics at the Johannes Kepler University Linz, Austria. He is currently working in the field of liquid sensors and monitoring systems.